ChemSusChem

Research Article
doi.org/10.1002/cssc.202201912

Chemistry Europe
European Chemical Societies Publishing

www.chemsuschem.org

VIP *Very Important Paper*

Accessing the Primary Solid–Electrolyte Interphase on Lithium Metal: A Method for Low-Concentration Compound Analysis

Bastian von Holtum,[a] Maximilian Kubot,[a] Christoph Peschel,[a] Uta Rodehorst,[a] Martin Winter,[a, b] Sascha Nowak,[a] and Simon Wiemers-Meyer*[a]

Despite large research efforts in the fields of lithium ion and lithium metal batteries, there are still unanswered questions. One of them is the formation of the solid – electrolyte interphase (SEI) in lithium-metal-anode-based battery systems. Until now, a compound profile analysis of the SEI on lithium metal was challenging as the amounts of many compounds after simple contact of lithium metal and the electrolyte were too low for detection with analytical methods. This study presents a novel approach on unravelling the SEI compound profile through accumulation in the gas, liquid electrolyte, and solid phase. The method uses the intrinsic behavior of lithium metal to spontaneously react with the liquid electrolyte. In combination with complementary, state-of-the-art analytical instrumentation and methods, this approach provides qualitative and quantitative results on all three phases revealing the vast variety of compounds formed in carbonate-based electrolytes.

Introduction

Enabling efficient energy storage and high energy density applications are just a few of the major motives in today's battery research and development. In this context lithium ion batteries play an important role since their commercial introduction in 1991.[1,2] Ever since, researchers have been working on improving this type of battery in terms of capacity, Coulombic efficiency, lifespan, safety, sustainability, and economic aspects.[3–6] However, the widely used electrode materials, being graphite on the anodic side and transition metal oxides and phosphates on the cathodic side still have their limitations.[7–11]

One possible path leading to higher energy densities is the development of rechargeable lithium metal battery (LMB) cells, utilizing lithium metal foil as the negative electrode material. This setting was introduced in the early 1970ies[12,13] This (re)development from graphite (370 mAh g^{-1}) to lithium metal (3860 mAh g^{-1}) would lead to an improvement by a factor of ten regarding the theoretical specific capacity of the anode material.[7]

Even so, issues with this kind of negative electrode were also discovered during the research and commercialization processes. The biggest issues are the growth of high surface area lithium (HSAL) deposition morphologies (often called after the most prominent morphology: dendritic) leading to low cycle life and safety hazards caused by high surface area and short circuits.[14–16] Further the low Coulombic efficiency of these cells due to a constant loss of active material and electrolyte should be noted.[17,18]

The term solid–electrolyte interphase (SEI) was first introduced by Peled in 1979.[19] In that study, some of the core characteristics of this phase were already identified and are still valid today. He claimed this layer to have properties of a solid electrolyte, being electron impermeable but ion conductive and consisting of rather insoluble reaction products.[19] Since then, several new aspects of the SEI were disclosed through research.[20,21] The constant growth of the SEI during cycling and the related issues of dendrite formation have been observed and tackled in many scientific publications, concerning the influence of the SEI properties on the formation of dendrites and vice versa.[14–16,22]

Even more studies focus on the analysis of species that the SEI consists of and how the overall morphology of this interphase looks like.[23–25] Time-of-flight secondary ion mass spectrometry (ToF-SIMS), transmission electron cryomicroscopy (cryo-TEM) and X-ray photoelectron spectroscopy (XPS) are just a few of the techniques that can be used in this context, but together these studies are not capable to describe the whole story about SEI formation as until today it is not possible to track all reactions and get all necessary information. Still piece by piece researchers try to create a holistic understanding of the SEI.[18]

This study will focus on the initial formation of the SEI even before any external current was applied. This SEI is formed

[a] B. von Holtum, M. Kubot, C. Peschel, U. Rodehorst, Prof. M. Winter, Dr. S. Nowak, Dr. S. Wiemers-Meyer
MEET Battery Research Center, University of Münster
Corrensstr. 46, 48149 Münster (Germany)
E-mail: simon.wiemers-meyer@uni-muenster.de
m.winter@fz-juelich.de

[b] Prof. M. Winter
Helmholtz Institute Münster, IEK-12
Forschungszentrum Jülich GmbH
Corrensstr. 46, 48149 Münster (Germany)

spontaneously due to the contact of bare and reactive lithium with the electrolyte. In prior reports, this phase has been given different names, including "primary",[26] "primitive",[18] or "initial" SEI.[27–29] In this study, it will be referred to as "primary SEI".

As this specific interphase is present in every lithium metal cell after assembly, it is logical to put effort into elucidating its composition. It represents a starting point for every lithium metal cell and depending on its composition will influence cell performance. Molecular structure elucidation of organic compounds originating from this primary SEI could not be tackled up to now, as the major difficulty of the primary SEI lies in the low thickness, which is in the lower nanometer scale. The associated low abundancy of analytes generally does not allow speciation analysis, for example with methods like gas chromatography or liquid chromatography coupled to mass spectrometry. NMR as well lacks the sensitivity at this state.

For this reason, a sample preparation method that allows to accumulate primary SEI formation products in the liquid electrolyte, the gas phase, and the solid phase inside of a closed sample environment is introduced. Even though in the context of lithium metal batteries, there are electrolytes exhibiting greater performances using for example fluoroethylene carbonate (FEC),[30] this study presents the proof-of-principle of this new method using an electrolyte consisting of 1.2 mol L^{-1} lithium hexafluorophosphate ($LiPF_6$) in ethylene carbonate (EC). Furthermore, it shows the results of its application on a well elaborated and simple carbonate-based electrolyte being 1.2 mol L^{-1} $LiPF_6$ in a mixture of EC and ethyl-methyl carbonate (EMC) in a solvent weight ratio of 3:7, which is commonly used in lithium-ion batteries.

Experimental Section

Materials

Lithium metal foil, with 50 µm thickness was purchased from Albemarle (North Carolina, USA). The electrolyte consisting of $LiPF_6$ (1.2 mol L^{-1}) EC/EMC (3:7 w/w) was gained from Tomiyama High Purity Chemicals (Tokyo, Japan). The electrolyte consisting of $LiPF_6$ (1.2 mol L^{-1}) and EC was prepared by combining the pure chemicals inside of an argon atmosphere glovebox by MBraun (Garching, Germany). $LiPF_6$ and EC, with purities over 99% were ordered from EMCHEM (Jecheon, South Korea).

Zirconium(IV)-oxide mill balls with 5 mm diameter were ordered from Fritsch (Idar-Oberstein, Germany) and the 10 mL cycloolefin copolymer (COP) -vials for sample preparation were obtained from Gerresheimer (Düsseldorf, Germany). Crimp caps with polytetrafluoroethylene (PTFE)/silicone septa were purchased by SCP (Weiterstadt, Germany).

Sample preparation

Lithium metal foil was prepared in a dry-room (dew point set to $< -65\,^{\circ}C$). It was first cut to a total area of 1000 mm^2 for each sample and accordingly cut into pieces of 2 mm width and 10 mm length in between mylar foil. The pure lithium stripes were then stored in COP-vials, which were packed into evacuated pouch bags for sample transport.

Inside of the inert argon atmosphere of a glovebox, the pouch bags were re-opened and 1000 µL of the distinct electrolyte, together with two mill balls were added to the COP-vials. The vials were then crimped and ready for treatment.

For sample treatment, the vials were put into a custom build sample holder attached to a vortexer unit by Scientific Industries (New York, USA). Using the maximum setting of 2700 rpm, samples were treated for 10 min up to 72 h depending on the experimental purpose.

As shown in Figure 1, this method is based on the spontaneous formation of the primary SEI, whenever bare lithium metal is in contact with the applied electrolyte (A).[19] The formation is followed by a treatment using zirconium(IV)-oxide mill balls, which physically destroy the interphase (B). After the destruction, lithium metal is again in direct contact with the electrolyte, forming a new primary SEI (C). Repeating this cycle from A to C will end up in the accumulation of all reaction products in the three aforementioned phases.

In the process of method development to achieve not only qualitative but quantitative results with the sample preparation method, modifications had to be made. The treatment duration was increased from several minutes to hours. Further the actual turnover of a standard carbonate-based electrolyte comprising of $LiPF_6$ (1.2 mol L^{-1}) in EC/EMC (3:7 w/w) was monitored. Within this experiment, samples were treated for 1, 6, 12 h and 24, 48 and 72 h. Samples rested for 24 h before measurements were performed on a gas chromatography (GC) barrier ionization discharge (BID) and thermal conductivity detection (TCD) system.[31] The injection volume of the sample was optimized to fit the range of the calibration by changing its volume in the range of 25 µL to 250 µL. An averaged value for the injection volume was not possible to be used in all cases, as the range of intensities of the observed species varied with treatment duration.

After quantitative gas analysis, the remaining electrolyte was transferred into a spin column system by Ahn (Nordhausen, Germany), centrifuged at 14.500 rpm for 10 min with a miniSpin plus by Eppendorf (Hamburg, Germany) and further used for liquid analysis using Nuclear magnetic resonance spectroscopy (NMR), solid phase micro extractions coupled with gas chromatography mass spectrometry (SPME-GC-MS), liquid chromatography coupled

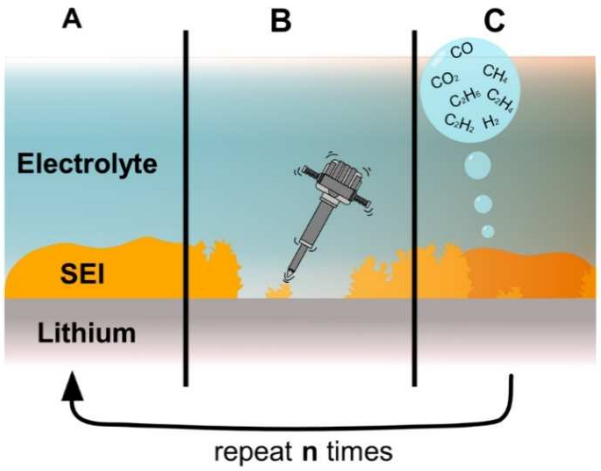

Figure 1. Schematic representation of primary SEI compound accumulation through spontaneous SEI growth (A), destruction by physical methods (B), and primary SEI reconstruction (C), resulting in compound accumulation due to continuous repetition of A – C.

with ion-trap time-of-flight mass spectrometer (LCMS-IT-ToF) and GC-TCD.

For any experiment on the solid phase, this phase was washed two time with 0.5 mL DMC and centrifuged for 10 min at 14.500 rpm. To dry the sample the spin column was centrifuged for 5 min at 14.500 rpm. Quantification of solid compounds was performed by adding the distinct solvent to a COP-vial in an argon atmosphere, sealing the vial and directly before measuring, 500 μL of either H_2O or HNO_3 were added with a syringe through the septum. The sample was vortexed for 30 s and the headspace was analyzed by GC-BID/TCD and NMR. The insoluble phase also is analyzed by X-ray powder diffraction (XRD).

Instrumentation and measurement parameters

Gas chromatography-mass spectrometry (GC-MS) experiments for proof-of-principle were executed on a Shimadzu GCMS-QP2010 Ultra with assembled AOC-5000 Plus autosampler (Shimadzu, Kyoto, Japan) and a nonpolar Supelco SLB-5 ms (30 m × 0.25 mm. 0.25 μm; Sigma Aldrich, Steinheim, Germany) column.

Quantitative GC measurements were carried out on a GC-2010 Plus system. For the quantification, a BID-2010 Plus and a TCD-2010 Plus detector were used (all Shimadzu, Kyoto, Japan). Injections were performed manually with a 0.5 mL or a 0.025 mL headspace-syringe. The system is controlled by the LabSolutions software (version 5.90) by Shimadzu (Kyoto, Japan). The resulting chromatograms were evaluated with the Postrun Analysis editor (version 5.90) from Shimadzu(Kyoto, Japan).[31] For chromatographic separation of the GC-BID measurements a PLOT gas separation column RT®-Msieve 5 A (30 m × 0.32 mm × 30 μm) and a packed RT®-ShinCarbon ST (80/100, 2.0 m × 0.53 mm for GC-TCD, both by Restek (Bad Homburg, Germany) were utilized. GC parameters and calibration were conducted and adapted according to Leißing et al., using a gas mix by Westfalen AG (Münster, Germany; Table 1) together with a gas mixing device (GMS-2CH by QCAL Messtechnik GMBH, Oberostendorf, Germany).[31]

All solid phase micro extractions (SPME) were performed with acrylate fibers in headspace mode. The sample was held at room temperature to prevent further aging of the electrolytes by thermal decomposition during the sampling procedure. The SPME setup from CTC Analytics (Zwingen, Switzerland) controlled by the cycle composer software of the AOC 5000 autosampler (Shimadzu, Kyoto, Japan) was used. SPME-GC-MS experiments were executed on a GCMS-QP2010 Ultra with assembled AOC-5000 Plus autosampler (Shimadzu, Kyoto, Japan) and a nonpolar Supelco SLB®-5 ms (30 m × 0.25 mm. 0.25 μm; Sigma Aldrich, Steinheim, Germany) column. Further parameters and sample preparation conditions were applied according to Horsthemke et al.[32]

Table 1. Composition of applied gas mix used for GC-BID and GC-TCD calibration. Calibration was performed according to Leißing et al.[31]

Component (purity)	Analytical value/V%
Butane (3.5)	1.00
Carbon dioxide (4.5)	0.98
Carbon monoxide (4.5)	0.99
Ethane (3.5)	1.01
Ethene (3.5)	1.00
Ethine (2.6)	1.01
Hydrogen (5.0)	1.02
i-Butane (2.5)	1.00
i-Pentane (2.5)	1.04
Methane (3.5)	1.01
Nitrogen (5.0)	1.03
Oxygen (5.0)	1.02
Propane (3.5)	1.00
Propene (3.5)	1.00
Argon (5.0)	Matrix

Nuclear magnetic resonance spectroscopy (NMR) experiments were performed employing an AVANCE III HD spectrometer by BRUKER (Massachusetts, USA) at 400 MHz (^{1}H) and a broadband probe (PA BBO 400 MHz, BRUKER). As no standard was added to the electrolytes, the signals of EC at 4.63 ppm (^{1}H) and 67.1 ppm (^{13}C) and the signals of PF_6^- at −72.2 ppm (^{19}F) and −146.1 ppm (^{31}P) were used as references, respectively. These chemical shifts were obtained from prior reports.[33] Although the reported electrolyte composition slightly differs, deviations of the chemical shifts are considered negligible. For the analysis of the solids, 500 μL of D_2O were added.

For LC–MS investigations, a Nexera X2 UHPLC system (Shimadzu, Kyoto, Japan) hyphenated to a liquid chromatography coupled with ion-trap time-of-flight mass spectrometer (LCMS-IT-ToF; Shimadzu, Kyoto, Japan) was used. Reversed-phase (RP) chromatography was conducted on a Poroshell 120 SB–C18 column (100 mm × 2.1 mm, 1.9 μm; Agilent Technologies, Santa Clara, USA) at 40 °C and a flow rate of 0.5 mL min^{-1} with acetonitrile and deionized water as eluents. Hydrophilic interaction liquid chromatography (HILIC) was performed using a Hypersil GOLD™ SAX column (200 mm × 2.1 mm, 1.9 μm, 175 Å Thermo Fisher Scientific, Massachusetts, USA) These measurements were performed at 40 °C and a flow rate of 0.35 mL min^{-1} with 10 mmol L^{-1} aqueous solution of ammonium formate (NH_4HCO_2) at pH 6.5 and acetonitrile. Further parameters and sample preparation were conducted according to Henschel et al.[34,35]

X-ray powder diffraction (XRD) measurements were performed on a Bruker D8 Advance X-ray powder diffractometer (Bruker AXS, Karlsruhe, Germany). The instrument runs on nickel filtered copper K_α radiation, with a wavelength of $\lambda = 0.154$ nm at 40 kV acceleration voltage and 40 mA current flow. The experiments were performed in a 2θ range between 10° and 90°, with a step size of around 0.02 s^{-1} and 2 s data collection time per step in continuous mode of the Lynxeye detector. The divergence slit of the detector was set to 0.6 mm, which resulted in sufficient intensities for the identification of phases of smaller amounts. Resulting reflexes were compared to data from PDF-2 library from Bruker.

Results and Discussion

Proof of principle

For verification of the effectiveness of the sample preparation method in accumulating SEI-derived compounds, different samples were compiled. These were treated two times for 10 min every 24 h, and then measured by GC-MS(Figure 2). The different samples were: The lithium blank (black), consisting of lithium metal stripes and two mill balls; the electrolyte blank (green) consisting of an $LiPF_6$ (1.2 mol L^{-1}) in EC electrolyte and two mill balls; the sample (red), consisting of lithium metal stripes, electrolyte and two mill balls; and the sample blank (blue), consisting of the same components as the latter but this was not treated to serve as a direct comparison.

The use of these four different samples assured that signals being observed on the GC-MS system can be traced back to a certain component of the samples, whether this is the electrolyte, the lithium metal, or the SEI formation. The formation of

the interphase on the lithium surface should be spontaneous as lithium metal (standard electrode potential of −3.040 V vs. the standard hydrogen electrode (SHE)) will exceed the electrochemical stability window of every organic carbonate-based electrolyte available, leading to degradation of the electrolyte components.[18,19,36] This degradation will spontaneously form the primary SEI.

As shown in Figure 2, the electrolyte blank (green) and the sample blank (blue) did not show any signals above the limit of detection (LOD). The lithium blank (black) showed one low intensity signal around 2.0 min representing hydrogen. This signal was later assigned to be the result of water residues, reacting with the lithium metal. In later experiments these residues were prevented by extensively drying of all relevant components of the experiments (sample containers, caps, and mill balls) at 60 °C under vacuum overnight.

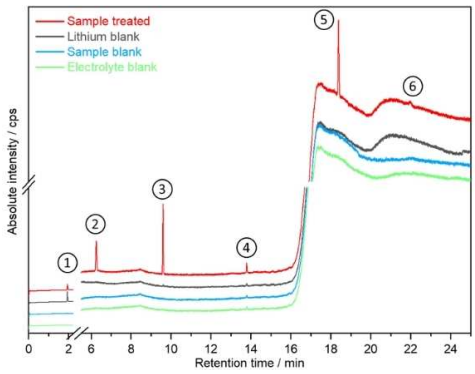

Figure 2. Total ion chromatograms (TICs) of GC-MS measurements of different samples, all containing the electrolyte $LiPF_6$ (1.2 mol L^{-1}) in EC for method validation; the electrolyte blank is shown in green, the lithium blank in black, the sample blank in blue, and the sample in red. The present gas species are hydrogen (1), methane (2), carbon monoxide (3), ethane (4), ethene (5), and ethine (6). The signals in the range of 2.5 min to 4.5 min were cut out because of the inevitable signals of nitrogen, oxygen and argon, reaching the detector limit.

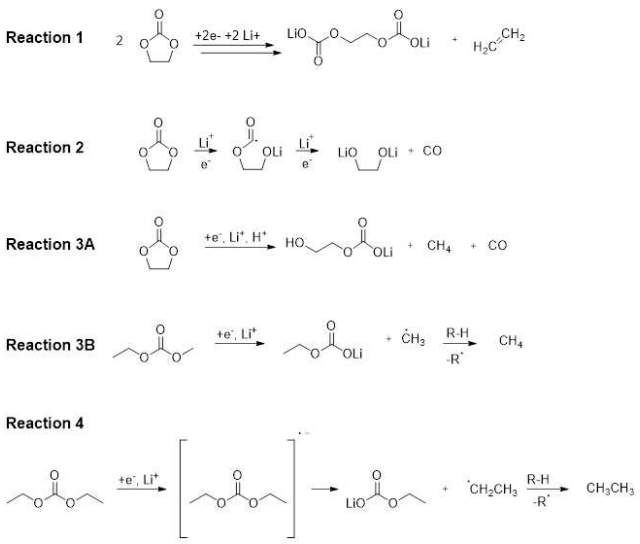

Figure 3. Formation of ethene (reaction 1),[37,39,40] carbon monoxide (reaction 2),[37–39] methane (reactions 3 A[41] and 3B[42]) and ethane (reaction 4).[42]

Apart from that, only the sample (red) indicated some signals, being methane at 6.25 min (2), carbon monoxide around 9.6 min (3), ethane at 13.8 min (4), ethene at 18.4 min (5) and ethine at 22.0 min (6). In the context of lithium-based batteries, those compounds have been observed in other studies before.[37,38]

The increase of ethene and carbon monoxide can be explained through a mechanism of the single electron transfer that was described by Aurbach et al., Shkrob et al., Mogi et al., and others (Figure 3, reactions 1 and 2).[37–40] Furthermore, the formation of methane and ethane is observed, but has not been described in detail for methane in the context of a purely EC-based carbonate electrolyte. In that case, the study reported by Hobold et al. can be taken into account (Figure 3, reaction 3 A).[41] In general, methane can be observed as a reduction product of EMC or DMC following the mechanism shown in Figure 3, reaction 3B.[42]

According to previous studies,[42,43] the occurrence of ethane reveals the same issue as methane. There are only studies that observed the occurrence of ethane in battery cell systems using EMC or DEC containing electrolytes. (Figure 3, reaction 3).

The results of this first experiment with a $LiPF_6$ in EC as electrolyte and the experimental setting serve as a proof-of-principle approach. All observed gaseous species are the result of the expected continuous formation of the primary SEI on lithium metal. In addition, these gases are in accordance with previously reported reaction mechanisms.

In the further course of this study, the results discussion will be presented according to the existing three phases: gaseous (permanent gases, light hydrocarbons), liquid (electrolyte) and solid (Li metal, SEI residues).

The gas phase

Expanding the treatment duration is found to result in higher absolute volumes of the respective gases (Figure 4B). These absolute volumes were calculated by using Equation (1):

$$V_{abs} = V_{Vial} \cdot \frac{V_{\%} \cdot V_{Inj}}{100 \cdot V_{cal}} \quad (1)$$

where V_{Vial} is the calculated volume of the COP vials, $V_{\%}$ is the determined percentage volume of the respective gas according to the calibration, V_{Inj} is the injected volume of the sample, and V_{cal} is the injection volume of the calibration (500 µL).

Observing these increased volumes on all treatment duration levels demonstrated that a complete turnover of all lithium metal, even if the solvent was triple in molar-excess, was not achievable in a reasonable timescale for the preparation-device and the related experimental design. The incomplete turnover was also confirmed by adding water to the sample still resulting in hydrogen formation visible through GC-BID measurements. Beside this, a complete turnover would have resulted in the observation of a plateau in the context of

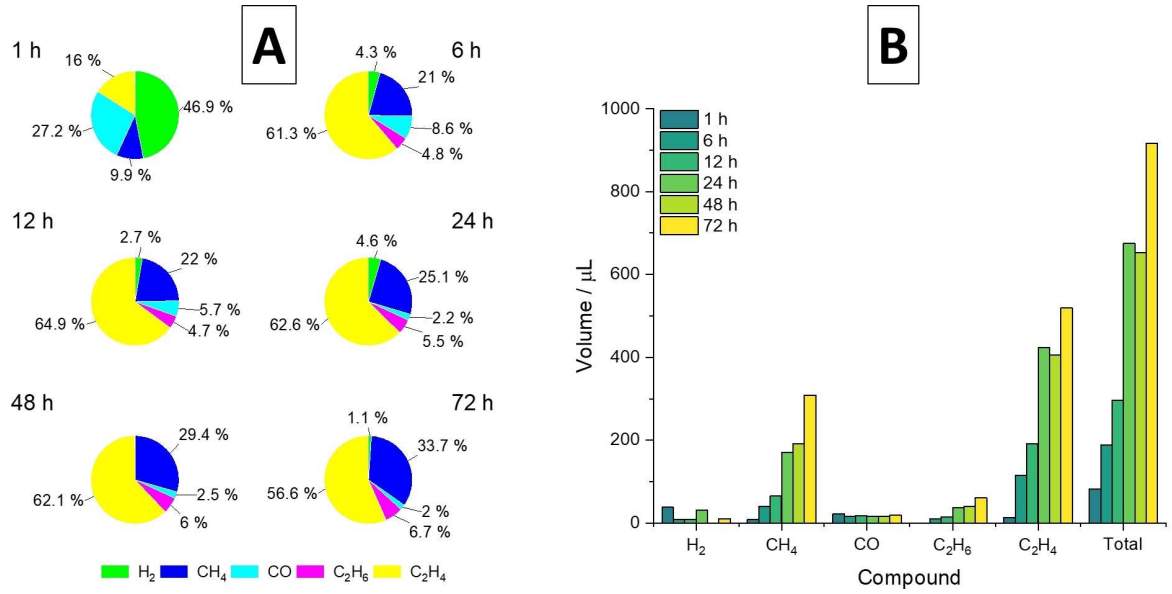

Figure 4. Relative (A) and absolute (B) amounts of gases measured with GC-BID and GC-TCD using the electrolyte $LiPF_6$ (1.2 mol L^{-1}) in EC/EMC (3:7 w/w) depending on treatment duration. Experimental deviations for this experiment were 0.1 % for the used electrolyte volume, 1 % for the used lithium metal foil and a manual injection error of 1 % during sampling.

the total gas volumes. This behavior implies that the absolute volumes cannot be used to interpret how much of one or all observed gases are formed by electrolyte reaction with a distinguished amount of metallic lithium. Furthermore, the influence of a pressure rise inside of the sample containers is not taken into account in all absolute results presented in this study. Instead, the relative amounts (Figure 4A) need to be used, as the reactions triggered by the constant destruction and reconstruction of the SEI are considered to be constant over the complete duration of the experiment, as the reactants are abundant in greater excess in contrast to the formed products. Therefore, the influences of the products are neglectable. This was also checked, comparing the constantly formed absolute volumes of CH_4, C_2H_6 and C_2H_4 over time. The presence of nitrogen and oxygen, which were cut out in the graphs, do not influence the quantification, as the calibration is based on the area of each individual peak of the calibration gas mix and not on the total area of the sum of all formed peaks.

Starting with hydrogen, it reveals constant low absolute levels without any ascending or descending trend but with the highest relative gas volume after 1 h of treatment. It seems to be a finite reaction caused by water impurities in the used electrolyte. As the level of hydrogen in the electrolyte blank is below the LOD, the reaction partner of water is lithium metal, but as the levels of hydrogen in the sample blank are below the LOD as well, the necessity of having fresh and reactive lithium metal surface instead of its lesser reactive form possessing a native passivation layer is highlighted. This reactive form is only provided by the preparation method.

For methane, an absolute and relative increase over time was observable. The reason for this could be the formation of methane following either reaction 3 A[41] or reaction 3B[42] in Figure 3.

Carbon monoxide was also formed at an early stage but was not formed any further, as visible in Figure 4. With regard to these results, the reported reactions (Figure 3, reactions 3 A and 3B of) cannot be interpreted as the source for methane, as both of them are based on carbonates which are abundant at all times and do not show any restriction that would explain the loss of its formation during the experiment. Therefore, the reaction forming carbon monoxide must be different.

In general, ethane demonstrated a slower formation reaction in comparison to ethene. These could be explained by the study of Seo et al.,[42] in which the formation of ethane is explained by single-electron transfer to a carbonate like EMC, forming a lithium alkyl carbonate and alkyl radical. The possibility of the alkene radical abstracting another hydrogen radical could then form ethane, but the authors also admitted that this last step is still not experimentally proven.

Ethene showed a decent increase over time. Ethene formation was studied in detail, describing the reductive EC decomposition.[37,39,40] Therefore, reaction 1 (Figure 3) forming LEDC and ethene out of EC via two single electron transfer reactions is a valid explanation.

In a next step, the same carbonate-based electrolyte was used for experiments applying a 12 h treatment. Firstly, this experiment was used for the same gas measurements as before to ensure method reproducibility. Secondly, this experiment was used for the electrolyte determinations using LCMS-IT-ToF, SPME-GC-MS and NMR. At last, the experiments provided the solid residues, which were further analyzed. Independent of the analytical phase of interest, the sample preparation and treatment were performed every time in triplicate.

The absolute and relative amounts of gas formed are given in Figure 5 and Table 2. The electrolyte formed on average 7 µL hydrogen, together with 14 µL ethane and 16 µL of carbon monoxide, as well as 64 µL methane and 190 µL ethene. The electrolyte formed on average 291 µL of gas with high reproducibility. All absolute and relative data values, together with standard deviations, are listed in Table 1.

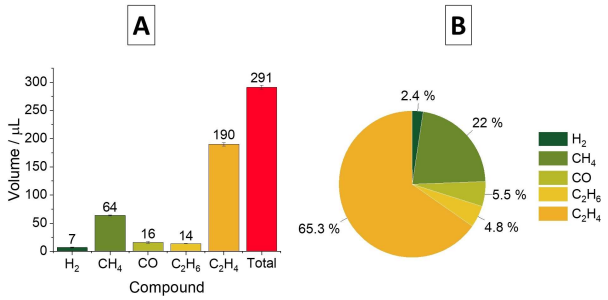

Figure 5. Absolute (A) and relative (B) results of the gas quantification by GC-BID and GC-TCD treated for 12 h in threefold determination.

Table 2. Average absolute and relative volumes of the gases formed due to constant primary SEI formation.

Gas species	Absolute volume [µL]	Relative standard deviation [%]	Relative amount [%]
H_2	7	0.87	2.4
CH_4	64	0.90	22.0
CO	16	1.63	5.5
C_2H_6	14	0.25	4.8
C_2H_4	190	2.94	65.3
Total	**291**	**3.25**	**100.0**

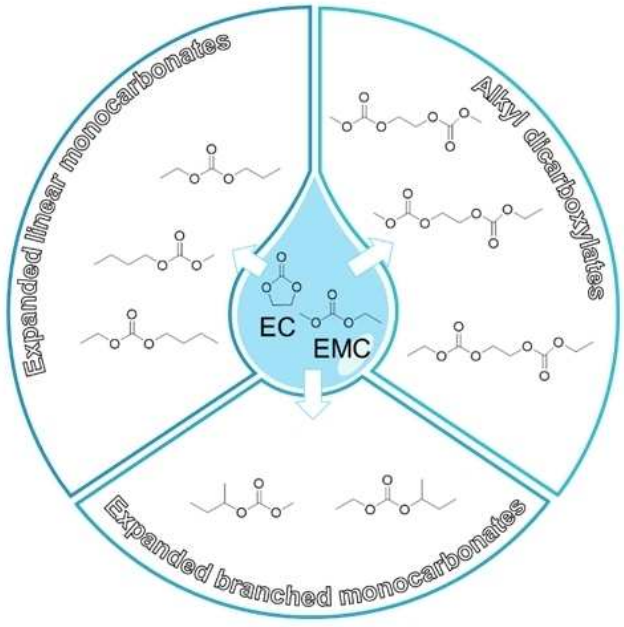

Figure 6. Identified carbonate-based compounds analyzed by SPME-GC-MS and assigned by comparison of MS-spectra with NIST11 library.

Concluding the results of the gas analysis, the novel sample preparation method allows an easy and reproducible way to investigate gassing reactions during this specific SEI formation for any kind of liquid electrolyte. In addition, the novel accumulation method can help to investigate the influence of specific electrolyte components during interphase formation.

The liquid electrolyte phase

Besides quantitative gas analysis, the electrolyte was filtered and studied by different chromatographic separation techniques coupled with mass spectrometry. SPME-GC-MS allows to analyze volatile molecules and identify them by comparison with an existing fragment database.[32] Three main groups of compounds were identified (Figure 6). These are the alkyl dicarboxylates, expanded linear carbonates and expanded branched carbonates. All three groups were described in prior reports, for example by Horsthemke et al.[32]

The three alkyl dicarboxylates dimethyl-2,5-dioxahexane dicarboxylate (DMDOHC), diethyl-2,5-dioxahexane dicarboxylate (DEDOHC) and ethylmethyl-2,5-dioxahexane dicarboxylate (EMDOHC) were already described in prior reports as the result of initial charging or aging in lithium-ion cells.[32,44,45] However, these compounds have never been observed in the context of the primary SEI formation without any applied current or voltage. By taking a look on the formation mechanism of the three compounds, as shown by Sasaki et al., it is comprehensible that these compounds could be formed in the performed experiments.[45]

Both the expanded linear and the expanded branched monocarbonates can be explained through the mechanism described by Horsthemke et al.[46] and Peschel et al.[43] The mechanism starts by single-electron transfer to a linear carbonate leaving an alkane radical. These radicals can then recombine with other carbonate-based radicals formed through H-abstraction or single electron transfer forming new carbon-carbon bonds of higher chain length.

Due to the presence of EMC in the electrolyte and therefore the possibility of having ethyl- and methyl-groups available for the formation of new carbon-carbon bonds there is a wide variety of possible reaction products. The five expanded monocarbonates shown in Figure 6 are the only compounds that were visible in yields that were reliably distinguishable from the noise in the extracted ion chromatogram (EIC) by a minimum ratio of 3:1.

In order to obtain more information about the oligocarbonates, which form during the primary SEI formation, HPLC-IT-ToF was used. Chromatography was performed either with RP or HILIC. Thus, being able to observe carbonate-based compounds and non-acidic organofluorophosphates through RP and acidic organofluorophosphates through HILIC measurements.

The results using RP or HILIC did not reveal any organofluorophosphates being formed through primary SEI formation. Meaning, that there was no signal of a compound above the noise level that at any point revealed accurate masses that

support the presence of phosphor. This demonstrates that during primary SEI formation, the formation of liquid products happens only by reaction of the organic carbonate solvents. These results are supported by the compound tables for organofluorophosphates of Henschel et al., which are the most detailed lists of those compounds reported to date and no matches for the accurate masses of this experiment could be found.[47]

Beside these results, several carbonate-based compounds were found and identified by MS^2 experiments in the reversed phase measurements. The total-ion chromatogram (TIC), with highlighted extracted ion chromatograms (EICs) are shown in Figure 7. All peaks in the TIC that have no highlighted EIC were either also part of the measured fresh electrolyte blanks or their structure could not be elucidated due to low abundance. The shown EICs do not allow any assumptions on their ratios or absolute abundance due to different ionization yields.

The proposed molecular structures are shown in Figure 8 together with their respective accurate masses, molecular ions and measured adducts. In addition, two other signals were observable, with an accurate mass of *m/z* 330.0992 and *m/z* 242.0863, forming $[M+Li]^+$ adducts. However, even with MS^2 fragmentation, a final molecular structure could not be proposed for both.

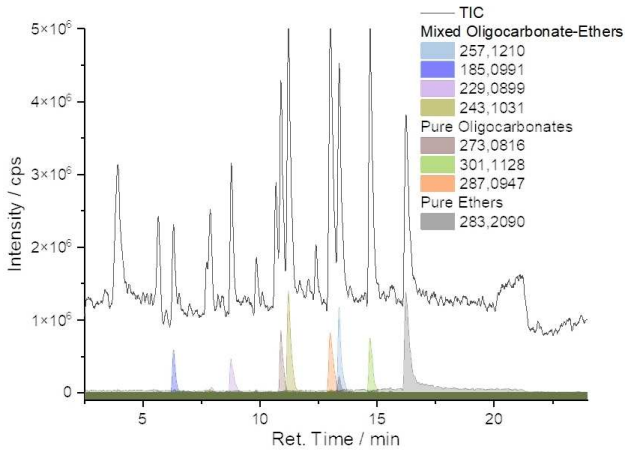

Figure 7. Total-ion chromatogram (black) and extracted-ion chromatograms (colors) of the electrolyte after 12 h treatment measured by RP-HPLC-IT-ToF.

The group of pure oligocarbonates consists of carbonate trimers having all possible ethyl- or methyl-terminal groups. Longer carbonates were not detectable. Compounds like these have already been reported in the context of lithium-ion batteries (LIB) by Henschel et al. also proposing a formation mechanism that leads to the observed compounds.[48] The only pure ether, with a mass of *m/z* 283.2090, has not been reported to date. The fact that only this one pure ether was detected could be the result of it being the longest one that was stable in the sample environment but also the smallest that was soluble, as these compounds are expected to be less soluble with increasing length. In this case, all longer pure ethers would be part of organic reflexes in XRD measurements. The novelty of this compound is the double bond in the terminal alkyl group. The existence and positioning of this bond was secured by MS^2 spectra.

The third group comprises of a mixture of compounds including ether and carbonate structures. Two of them with exact masses of *m/z* 229.0899 and *m/z* 243.1031 could not be identified completely, as the MS^2 spectra does not allow the exact positioning of the ether group inside of the molecule due to unspecific fragment ions. Therefore, all possible molecular structures are presented for these two masses in Figure 8. However, the possibility of having the ether group at a terminal position is higher due to elongation mechanism.[45,48] The compound with an exact mass of *m/z* 257.1210 was already reported and elucidated by Henschel et al.[48] The last member of this group with *m/z* 185.0991 exact mass having a terminal hydroxy group was not reported to date.

Finally, the processed electrolytes were analyzed by NMR spectroscopy to establish the stability of the conducting salt. The ^{19}F and ^{31}P spectra (Figure 9), show only the doublet for PF_6^- at −72.7 ppm (^{19}F) and the septet at −146.1 ppm (^{31}P) both with a coupling constant of 708 Hz. No other signal is

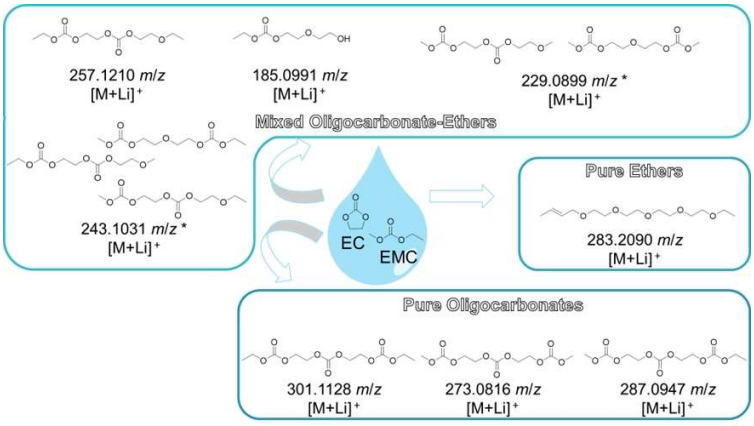

Figure 8. Carbonate-based structures identified by MS^2 experiments using RP-HPLC-IT-ToF. These were divided into three main groups: mixed oligocarbonate ethers, pure ethers, and pure oligocarbonates.

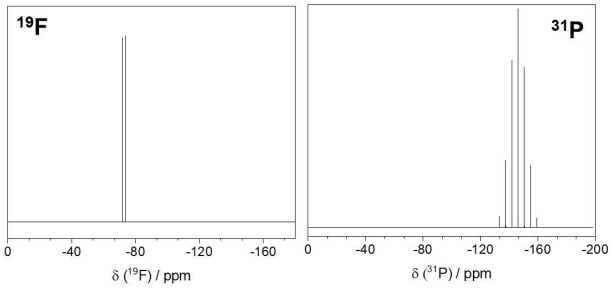

Figure 9. Liquid NMR spectra of the electrolyte after 12 h of treatment. Left: ^{19}F spectrum; right: ^{1}P spectrum, both showing solely the signals of PF_6^-.

observable over the complete spectral width, concluding that the conducting salt $LiPF_6$ is not contributing to the primary SEI formation in the form of electrolyte soluble compounds. In addition, its presence without hints on its degradation products indicates a non-acidic environment in which $LiPF_6$ is stable. These results can be helpful for any kind of simulation study on interphase formation in lithium-based batteries, as it simplifies the reaction mechanism network due to the missing involvement of the conducting salt.[49]

In summary, the results for the analysis of the liquid electrolyte phase reveal a wide variety of compounds that so far only have been observed in the context of LIBs but have never been observable in a study concerning the primary SEI formation on lithium metal (i.e., in LMBs). Therefore, the accumulation method reveals to be a valid method to study the starting point of any kind of liquid electrolyte that is supposed to be in contact with lithium metal in a battery cell. The compounds identified by SPME-GC-MS focusing on small, more volatile molecules and RP-HPLC-IT-ToF enabling the analysis of the soluble carbonate-based compounds collectively allow to give small insights into ongoing reactions in the electrolyte, that for example create higher oligocarbonates starting from dicarboxylates like DMDOHC or go in a different direction after the dicarboxylates introducing ether groups to the molecular structures. Furthermore, the results point out the low reactivity of the conducting salt $LiPF_6$ during primary SEI formation.

The solid phase

As an approach on gathering information on the solid residues of the experiment, which should contain the accumulated primary SEI, two different experiments were made. One by adding deuterium enriched water (D_2O) to the dried solid ending up in a solution which can be used for NMR. Afterwards the water insoluble and hardly soluble solid remains were dried and investigated using XRD. Secondly, the dried solid residues of the experiment were used to quantify the amounts of carbonates, such as lithium carbonate (Li_2CO_3) and other acid-sensitive compounds like oligocarbonates or mixed-oligocarbonates, by adding nitric acid and quantifying the produced carbon dioxide with GC-TCD as well as the amount of lithium carbide (Li_2C_2) by adding deionized water and quantifying the produced ethine using the GC-BID technique.

The ^{19}F spectrum of the sample dissolved in D_2O shows two signals that can be assigned to PF_6^- at −72.7 ppm with a coupling constant of 708 Hz and a singlet at −128.5 ppm (Figure 10). For identification of this signal, sodium fluoride was added to the sample. The signal at −128.5 ppm is not observable anymore, but another significantly more intense singlet at −123.5 ppm originating from fluoride is visible. Therefore, the small singlet is assigned to fluoride, as it is possible to shift its position in the spectra, as a result of concentration differences of the fluoride.

In the XRD pattern (Figure 11), three different species could be assigned. The highest share belongs to two crystalline organic substrates around $2\theta = 14°$ and 28°. The PDF-2 library by Bruker was not capable of giving any reasonable results for a certain compound for these reflexes besides the essence of it both being of pure organic nature. Furthermore, lithium carbonate was identified, being the

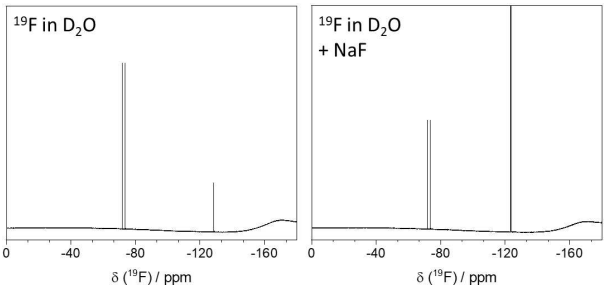

Figure 10. Liquid NMR spectra of aqueous solutions obtained by adding pure D_2O to the dried solid phase of the experiment. Left: ^{19}F spectrum; right: ^{19}F spectrum after the addition of sodium fluoride.

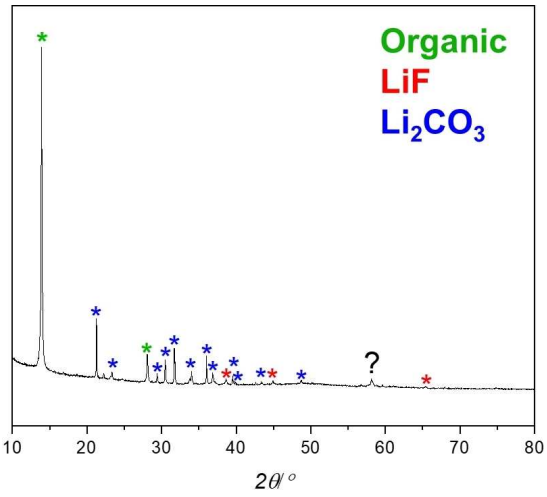

Figure 11. XRD pattern of the water insoluble components of the solid phase of the experiment, using PDF-2 library for reflex identification. Showing mainly crystalline organic reflexes (green), lithium carbonate (blue) and traces of lithium fluoride (red), together with an unidentifiable reflex around $2\theta = 58°$.

result of various reactions of the organic carbonates EC and EMC.[50,51] Additionally, small reflexes of lithium fluoride (LiF) could be assigned, which supposed to be the rests of the LiF not being able to dissolve in the D_2O used for the NMR measurements, due to poor solubility There was only one small reflex around $2\theta = 58°$, that could not be assigned to any of the library data.

The results of the solid phase were in accordance with previous studies,[52–54] where the general SEI of a simple lithium-metal-based battery containing a carbonate-based electrolyte with $LiPF_6$ as conducting salt and without any electrolyte additives, was expected to include significant amounts of organic decomposition products, probably containing higher oligo- or even polycarbonates or -ethers together with lithium carbonate as an inorganic decomposition product. According to prior reports, and especially those on simulations of primary SEI formation, the share of lithium fluoride was expected to be higher, owing to the favorable decomposition of the conducting salt in contact with lithium metal.[49] However, the results of this study show relatively low amounts of lithium fluoride and, together with the analysis of the liquid electrolyte phase, it can be stated that the reactivity of $LiPF_6$ during primary SEI formation is low, maybe even negligible.

Two compounds out of the solid residues were quantified utilizing GC-BID and GC-TCD methods. Firstly. The reaction of carbonates with nitric acid towards the production of carbon dioxide was used in the GC-TCD setting. A threefold determination for quantification showed 133 µL of CO_2 per mg solid residue with an error of ± 5 µL mg^{-1}. By performing the same experiment with fresh electrolyte and electrolyte of a 12 h treated sample, we discerned that the measured gas originated from carbonates, except the electrolyte solvents EC and EMC and soluble carbonates presented in Figures 6 and 8. The fresh electrolyte did not form quantifiable volumes of CO_2 in the time range of the experiment with solid residues, but the treated electrolyte formed CO_2. We suppose that the CO_2 from the electrolyte after treatment is formed through acid-sensitive compounds for example oligocarbonates. Furthermore, measurements of the solid residues with nitric acid and GC-BID analysis showed quantifiable amounts of methane and carbon monoxide. Methane can arise out of semi- or oligocarbonates or other carbonates with organic functional groups with HNO_3 as reaction partner underlining the XRD results with intense reflexes for organic compounds. Therefore, we assign the formed carbon dioxide of the solid residues measured with GC-TCD to electrolyte/HNO_3 insoluble but acid-sensitive organic oligo and semi-carbonates and inorganic carbonates like Li_2CO_3. In addition, NMR analysis of the HNO_3 and H_2O solutions of the solid residues and the DMC wash solutions were performed but no compound that would be the result of semi- or oligocarbonates reacting with nitric acid, like ethanol or methanol were detectable, which can be explained by solely gaseous reaction products like methane, carbon monoxide and carbon dioxide. As this study does not allow any structure elucidation of on the organic compounds in the solid residue, the reason why only methane was quantifiable but ethane as the product of ethyl-group reaction with nitric acid was below the limit of quantification remains uncertain.

Secondly, the amount of lithium carbide in the solid phase was quantified by GC-BID, as ethine after water addition to the solid in the same experimental setting as the latter. In this experimental environment, only carbide should react to ethine after water addition. Doing so, 5 wt% $\pm$ 3 wt% of Li_2C_2 in the solid phase have been detected. In order to assure that the carbide is formed in the context of the experiment and is not part of the lithium metal in terms of a production contamination occurring through molten salt lithium metal production over graphite rods, lithium metal was investigated separately in parallel, but no ethine formation was observed.[55]

The quantification of inorganic primary SEI components is a novel approach and contributes first data on the amounts of those compounds in this specific interphase (SEI) together with the elemental lithium remains. The presence of lithium carbide in the SEI in general was already reported, but no quantitative values were given.[56–59] Our experiments lead to the assumption that lithium carbide could be more stable in the environment of the primary SEI. As soon as a current is applied, it could have the possibility to behave differently, resulting for example in ethine formation through hydrogen abstraction. This could lead to levels of carbide which are near or below the limit of detection of state-of-the-art analytical methods explaining the different reports on its existence in the SEI after cycling.[56–59]

Conclusion

Quantitative analysis on the formation of the primary SEI and composition of this interphase faces the problem that the amount of many compounds is too low to detected by current analytical methods. This study presents a proof-of-principle and application of a new method that enables the accumulation of primary SEI formation products formed on lithium metal by using a standard carbonate-based electrolyte and contributes to molecular structure elucidation and quantification of those compounds by using complementary state-of-the-art analytical methods.

Furthermore, this method significantly improves the detectability of species from the emerging gas phase, soluble in the electrolyte, or present in the solid phase, including the primary SEI. Species were analyzed qualitatively and, in the cases of directly emerging gases during primary SEI formation and later during the investigation of the solid residues focusing on electrolyte/HNO_3 insoluble organic semi- and oligocarbonates, together with inorganic carbonates like lithium carbonate through GC-TCD analysis and lithium carbide with GC-BID analysis even quantitatively. In addition, the quantification of permanent gases and their standard deviations supported the reproducibility of the accumulation method, making it suitable for primary SEI studies using liquid electrolytes.

The experimental results revealed a vast variety of compounds that form during primary SEI formation as a result of direct contact between lithium metal and the electrolyte, which inevitably happens in every lithium metal battery after assembly. Even if most of the species that were observed in this study are not new to the field of battery research, in the context of the primary SEI, this novel comprehensive methodology is a next step towards a holistic understanding of the primary SEI on lithium metal.

Acknowledgements

The authors want to thank the German Federal Ministry of Education and Research for funding the project "Lillint" (03XP0225E). Furthermore, the first author wants to thank Steffen Samlert for introducing the GC-MS system for the proof-of-principle measurements and the workshop group of the Institute of Physics (University of Münster) for manufacturing the sample holder used for the accumulation method. Open Access funding enabled and organized by Projekt DEAL.

Conflict of Interest

The authors declare no conflict of interest.

Data Availability Statement

The data that support the findings of this study are available from the corresponding author upon reasonable request.

Keywords: batteries · lithium · mass spectrometry · NMR spectroscopy · solid–electrolyte interphases

[1] K. Ozawa, *Solid State Ionics* **1994**, *69*, 212–221.
[2] A. Yoshino, K. Sanechika, T. Nakajima (Asahi Kasei Corp., Tokyo) US4668595 A, **1986**.
[3] T. Kim, W. Song, D.-Y. Son, L. K. Ono, Y. Qi, *J. Mater. Chem. A* **2019**, *7*, 2942–2964.
[4] B. Liu, J.-G. Zhang, W. Xu, *Joule* **2018**, *2*, 833–845.
[5] M. Li, J. Lu, Z. Chen, K. Amine, *Adv. Mater.* **2018**, e1800561.
[6] S. Dühnen, J. Betz, M. Kolek, R. Schmuch, M. Winter, T. Placke, *Small Methods* **2020**, *4*, 2000039.
[7] X.-B. Cheng, R. Zhang, C.-Z. Zhao, F. Wei, J.-G. Zhang, Q. Zhang, *Adv. Sci.* **2016**, *3*, 1500213.
[8] H. Zhang, Y. Yang, D. Ren, L. Wang, X. He, *Energy Storage Mater.* **2021**, *36*, 147–170.
[9] A. Manthiram, *Nat. Commun.* **2020**, *11*, 1550.
[10] Y. Xia, J. Zheng, C. Wang, M. Gu, *Nano Energy* **2018**, *49*, 434–452.
[11] J. Yan, X. Liu, B. Li, *RSC Adv.* **2014**, *4*, 63268–63284.
[12] J. S. Dunning, W. H. Tiedemann, L. Hsueh, D. N. Bennion, *J. Electrochem. Soc.* **1971**, *118*, 1886.
[13] M. S. Whittingham (ExxonMobil Research and Engineering Co., Irving, TX), US 4009052 A, **1977**.
[14] D. R. Ely, R. E. García, *J. Electrochem. Soc.* **2013**, *160*, A662–A668.
[15] J.-I. Yamaki, S.-I. Tobishima, K. Hayashi, K. Saito, Y. Nemoto, M. Arakawa, *J. Power Sources* **1998**, *74*, 219–227.
[16] E. Cha, J. H. Yun, R. Ponraj, D. K. Kim, *Mater. Chem. Front.* **2021**, *5*, 6294–6314.
[17] J. Xiao, Q. Li, Y. Bi, M. Cai, B. Dunn, T. Glossmann, J. Liu, T. Osaka, R. Sugiura, B. Wu, J. Yang, J.-G. Zhang, M. S. Whittingham, *Nat. Energy* **2020**, *5*, 561–568.
[18] H. Wu, H. Jia, C. Wang, J.-G. Zhang, W. Xu, *Adv. Energy Mater.* **2021**, *11*, 2003092.
[19] E. Peled, *J. Electrochem. Soc.* **1979**, *126*, 2047–2051.
[20] E. Peled, D. Golodnitsky, G. Ardel, *J. Electrochem. Soc.* **1997**, *144*, L208-L210.
[21] M. Winter, *Z. Phys. Chem.* **2009**, *223*, 1395–1406.
[22] X. Wang, W. Zeng, L. Hong, W. Xu, H. Yang, F. Wang, H. Duan, M. Tang, H. Jiang, *Nat. Energy* **2018**, *3*, 227–235.
[23] H. Ota, K. Shima, M. Ue, J.-I. Yamaki, *Electrochim. Acta* **2004**, *49*, 565–572.
[24] A. C. Thenuwara, P. P. Shetty, M. T. McDowell, *Nano Lett.* **2019**, *19*, 8664–8672.
[25] H. Kuwata, H. Sonoki, M. Matsui, Y. Matsuda, N. Imanishi, *Electrochemistry* **2016**, *84*, 854–860.
[26] E. Peled, S. Menkin, *J. Electrochem. Soc.* **2017**, *164*, A1703–A1719.
[27] H. S. Dhattarwal, Y.-W. Chen, J.-L. Kuo, H. K. Kashyap, *J. Phys. Chem. B* **2020**, *124*, 27495–27502.
[28] K. Huang, S. Bi, B. Kurt, C. Xu, L. Wu, Z. Li, G. Feng, X. Zhang, *Angew. Chem. Int. Ed.* **2021**, *60*, 19232–19240; *Angew. Chem.* **2021**, *133*, 19381–19389.
[29] R. Xu, X. Shen, X.-X. Ma, C. Yan, X.-Q. Zhang, X. Chen, J.-F. Ding, J.-Q. Huang, *Angew. Chem. Int. Ed.* **2021**, *60*, 4215–4220; *Angew. Chem.* **2021**, *133*, 4261–4266.
[30] X.-Q. Zhang, X.-B. Cheng, X. Chen, C. Yan, Q. Zhang, *Adv. Energy Mater.* **2017**, *27*, 1605989.
[31] M. Leißing, M. Winter, S. Wiemers-Meyer, S. Nowak, *J. Chromatogr. A* **2020**, 461122.
[32] F. Horsthemke, A. Friesen, X. Mönnighoff, Y. P. Stenzel, M. Grützke, J. T. Andersson, M. Winter, S. Nowak, *RSC Adv.* **2017**, *7*, 46989–46998.
[33] S. Wiemers-Meyer, M. Winter, S. Nowak, *Phys. Chem. Chem. Phys.* **2016**, *18*, 26595–26601.
[34] J. Henschel, C. Peschel, F. Günter, G. Reinhart, M. Winter, S. Nowak, *Chem. Mater.* **2019**, *31*, 9977–9983.
[35] J. Henschel, J. L. Schwarz, F. Glorius, M. Winter, S. Nowak, *Anal. Chem.* **2019**, *91*, 3980–3988.
[36] I. Cekic-Laskovic, N. von Aspern, L. Imholt, S. Kaymaksiz, K. Oldiges, B. R. Rad, M. Winter, *Electrochemical Energy Storage* **2019**, 1–64.
[37] R. Mogi, M. Inaba, Y. Iriyama, T. Abe, Z. Ogumi, *J. Power Sources* **2003**, *119–121*, 597–603.
[38] I. A. Shkrob, Y. Zhu, T. W. Marin, D. Abraham, *J. Phys. Chem. B* **2013**, *117*, 19255–19269.
[39] L. Wang, A. Menakath, F. Han, Y. Wang, P. Y. Zavalij, K. J. Gaskell, O. Borodin, D. Iuga, S. P. Brown, C. Wang, K. Xu, B. W. Eichhorn, *Nat. Chem.* **2019**, *11*, 789–796.
[40] D. Aurbach, B. Markovsky, A. Shechter, Y. Ein-Eli, H. Cohen, *J. Electrochem. Soc.* **1996**, *143*, 3809–3820.
[41] G. M. Hobold, A. Khurram, B. M. Gallant, *Chem. Mater.* **2020**, *32*, 2341–2352.
[42] D. M. Seo, D. Chalasani, B. S. Parimalam, R. Kadam, M. Nie, B. L. Lucht, *ECS Electrochem. Lett.* **2014**, *3*, A91-A93.
[43] C. Peschel, F. Horsthemke, M. Leißing, S. Wiemers-Meyer, J. Henschel, M. Winter, S. Nowak, *Batteries & Supercaps* **2020**, *3*, 1183–1192.
[44] H. Yoshida, T. Fukunaga, T. Hazama, M. Terasaki, M. Mizutani, M. Yamachi, *J. Power Sources* **1997**, *68*, 311–315.
[45] T. Sasaki, T. Abe, Y. Iriyama, M. Inaba, Z. Ogumi, *J. Power Sources* **2005**, *150*, 208–215.
[46] F. Horsthemke, A. Friesen, L. Ibing, S. Klein, M. Winter, S. Nowak, *Electrochim. Acta* **2019**, *295*, 401–409.
[47] J. Henschel, S. Wiemers-Meyer, M. Diehl, C. Lürenbaum, W. Jiang, M. Winter, S. Nowak, *J. Chromatogr. A* **2019**, *1603*, 438–441.
[48] J. Henschel, C. Peschel, S. Klein, F. Horsthemke, M. Winter, S. Nowak, *Angew. Chem. Int. Ed.* **2020**, *59*, 6128–6137; *Angew. Chem.* **2020**, *132*, 6184–6193.
[49] J. Wagner, M. Gerasimov, F. Röder, P. B. Balbuena, U. Krewer, *Meet. Abstr.* **2021**, *MA2021-02*, 181.
[50] V. A. Agubra, J. W. Fergus, *J. Power Sources* **2014**, *268*, 153–162.
[51] A. M. Haregewoin, E. G. Leggesse, J.-C. Jiang, F.-M. Wang, B.-J. Hwang, S. D. Lin, *Electrochim. Acta* **2014**, *136*, 274–285.
[52] Z. Liu, P. Lu, Q. Zhang, X. Xiao, Y. Qi, L.-Q. Chen, *J. Phys. Chem. Lett.* **2018**, *9*, 5508–5514.
[53] S.-P. Kim, A. C. van Duin, V. B. Shenoy, *J. Power Sources* **2011**, *196*, 8590–8597.

[54] P. Zhai, L. Liu, X. Gu, T. Wang, Y. Gong, *Adv. Energy Mater.* **2020**, *10*, 2001257.
[55] R. Schmitz, R. Müller, S. Krüger, R. W. Schmitz, S. Nowak, S. Passerini, M. Winter, C. Schreiner, *J. Power Sources* **2012**, *217*, 98–101.
[56] E. Peled, D. Golodnitsky, A. Ulus, V. Yufit, *Electrochim. Acta* **2004**, *50*, 391–395.
[57] M.-S. Song, R.-H. Kim, S.-W. Baek, K.-S. Lee, K. Park, A. Benayad, *J. Mater. Chem. A* **2014**, *2*, 631–636.
[58] S. Konar, U. Häusserman, G. Svensson, *Chem. Mater.* **2015**, *27*, 2566–2575.
[59] L. A. Shimp, J. A. Morrison, J. A. Gurak, J. W. Chinn, R. J. Lagow, *J. Am. Chem. Soc.* **1981**, *103*, 5951–5953.

Manuscript received: October 14, 2022
Revised manuscript received: December 6, 2022
Accepted manuscript online: January 3, 2023
Version of record online: February 1, 2023